

Contents lists available at ScienceDirect

Acta Materialia

journal homepage: www.elsevier.com/locate/actamat



Full length article

Enhanced subsurface grain refinement during transient shear-based surface generation



Saurabh Basu, Zhiyu Wang, Ryan Liu, Christopher Saldana*

George W. Woodruff School of Mechanical Engineering, Georgia Institute of Technology, 801 Ferst Dr, Atlanta, GA, USA

ARTICLE INFO

Article history: Received 1 March 2016 Received in revised form 20 May 2016 Accepted 14 June 2016

Keywords: Strain path changes Crystallographic texture Information entropy

ABSTRACT

The present work combines quantitative orientation imaging microscopy and in situ digital image correlation to identify heterogeneities in the coupled mechanics and microstructure evolution occurring in the deformed subsurface during transient shear-based surface generation. Subsurface microstructure exhibited heterogeneities in terms of thickness of the ultrafine-grained layer and recrystallization fraction as a function of position along the surface wavelength. It was observed that subsurface microstructure evolution followed accelerated recrystallization kinetics due to strain path changes occurring in the subsurface during transient surface generation. The magnitudes of these strain path changes and prestraining of the deformed subsurface were observed to correlate well with changes in the information entropy of the corresponding subsurface crystallographic textures. A phenomenological model for predicting the information entropy of the orientation distribution function based on strain path changes and strain history was formulated and validated for monotonic loading paths. The implications of this generalized framework for modeling and controlling subsurface microstructure in transient surface generation are briefly discussed.

© 2016 Acta Materialia Inc. Published by Elsevier Ltd. All rights reserved.

1. Introduction

Functional response at interfaces of structural components is often strongly related to surficial topography and the corresponding microstructural state prevailing in the subsurface. For example, graded nano-scale microstructures characterized by grain size $\delta < 0.5$ um on biomedical implant surfaces has been shown to enhance biocompatibility due to grain boundary effects on tissue integration [1]. Significant attention has been made to understand relationships between functional response and surficial microstructure/topography with the overarching goal of designing optimal engineered surfaces constituting a balance of both of these surface parameters. To this end, studies that delineate microstructural influences on response have been performed on topographically featureless surfaces [2]. Through these studies, it was shown that nanocrystalline, nanotwinned and ultra fine grain (UFG) microstructures exhibit better corrosion response [3], fatigue resistance [4] and thermal stability [5], respectively. Complimentary to these studies, single variable functional response of

Corresponding author.

E-mail address: christopher.saldana@me.gatech.edu (C. Saldana).

topographically feature rich surfaces have showed direct correlation between surface topography and performance measures such as bio-compatibility [6] and wear [7].

Research motivated towards enhancing functional response has been augmented with studies that aim to simultaneously control surface microstructure and topography. In this regard, thermal ablation using precisely controlled high energy laser or electron beams has been realized as a technique to imprint controlled topographical feature arrays [8,9], as well as controlled microstructural characteristics [10]. While these techniques provide capability for high spatial resolution and precision, scalable implementation for controlled surface design is severely hampered by the high cost of capital equipment. In comparison, shear-based surface generation using transient material removal processes offers a scalable alternative for integrating sophisticated microstructural and topographical designs into fabricated components [7,11]. This process involves advancing a wedge shaped tool across a work surface in a periodic manner so to control the engagement and disengagement of the tool from the work surface. The resulting effect is a continuously varying surface topography which can be harnessed to yield a range of surface designs, including micro-scale ribs, fins and dimples [7,11]. While considerations pertaining to surface topography control have been well addressed, the integrated surface mechanics and microstructure consequences are not as well understood.

Microstructure evolution as a result of severe shear imposed in conventional surface generation involves interplay of dislocation storage and annihilation [12,13], sometimes compounded by twinning [14] and often resulting in UFG and nanocrystalline microstructures. This evolution is determined by the imposed thermomechanical state $(\varepsilon, \dot{\varepsilon}, T)$ and corresponding process parameters including tool geometry, deformation rate and deformation volume [15,16]. Surface generation occurring in conventional material removal involves deformation by severe simple shear $\varepsilon \gg 1$, resulting in spatially heterogeneous mechanics and microstructure evolution in the subsurface [17]. For transient material removal processes wherein operative process parameters are temporallyvarying, spatial and temporal heterogeneity of mechanics and microstructure evolution are not as well understood. Macroscopic consequences of variation in process parameters include continuously varying forces [18] and specific energy of deformation [19]. However, implications of transient material removal on surficial microstructure characteristics are yet to be elucidated.

Of particular interest in transient material removal processes are effects of strain path changes imposed in the work surface by the periodic tool engagement/disengagement on subsurface microstructure evolution. Strain path changes cause altered grain refinement rates $\left|\frac{\partial \delta}{\partial c}\right|$, crystallographic textures, continuous dynamic recrystallization (CDRX) statistics, grain boundary orientations and grain morphologies. For instance, CDRX of FCC metals and alloys has been observed to occur in an accelerated manner as a result of shear imposed in different directions in equal channel angular pressing (ECAP) [20-22]. This resulted in larger grain refinement rates $\left|\frac{\partial \delta}{\partial s}\right|$ compared with monotonic deformation paths at similar imposed effective strains ε . In the present study, evolution of microstructure and crystallographic texture during transient surface generation in OFHC Cu was investigated. From the present results, a phenomenological framework for predicting mechanics of microstructure evolution in transient surface deformation is discussed.

2. Experimental methods

A two-dimensional plane strain configuration shown in Fig. 1 was used to generate deformed surfaces in annealed OFHC Cu (grain size $\delta \sim 50~\mu m$). Control of the surface waveform was facilitated by advancing a hardened steel tool into the workpiece at a constant lateral velocity (X-direction) of $v_x = 25~mms^{-1}$ while sinusoidally modulating the tool vertical velocity (Y-direction) as $v_y(x) = 0.314 v_x \cos\left(\frac{2\pi x}{0.15}\right)~mms^{-1}$, in the range $v_y = [-7.9,7.9]~mms^{-1}$. The resulting surface waveform was given by $a_0(x) = 0.1 + 0.0075 \sin\left(\frac{2\pi x}{0.15}\right)~where all dimensions are in$

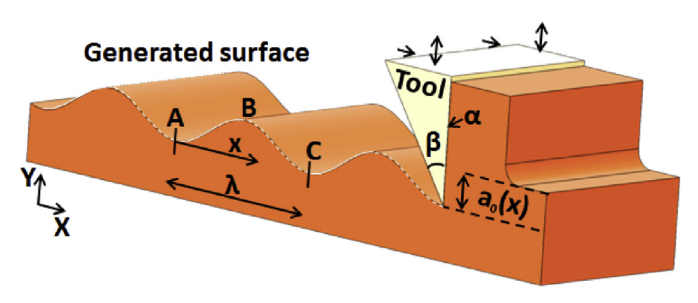


Fig. 1. Experimental configuration for transient surface generation.

mm. The tool had a nominal rake angle of $\alpha = 0^{\circ}$, an included angle of $\beta = 30^{\circ}$ and a clearance angle of $90^{\circ} - \beta = 60^{\circ}$. The effective rake angle varied continuously along the surface wavelength due to the imposed sinusoidal vertical velocity. The effective rake angle is related to the ratio of the lateral and vertical velocities as $\alpha_{eff}=-\tan^{-1}\left(\frac{\nu_y}{\nu_x}\right)$ which, for the present conditions, varied over the range $\alpha_{eff}=[-17.44^\circ,17.44^\circ]$. Additionally, several conventional surface generation experiments were also conducted with $v_{\nu} = 0$ to enable in situ characterization of the deformation field. In situ characterization of the deformation zone during surface generation was facilitated using digital image correlation (DIC). DIC involves recording material flow in the deformation zone in a sequence of digital images and subsequently using an image correlation algorithm to characterize the resulting displacement fields. Prior utilization of this technique has proven to be valuable for characterizing deformation fields in a broad class of deformation configurations [23-26]. Quantitative orientation imaging microscopy (OIM) of the material state left in the wake of the tool was performed using electron back-scattered diffraction (EBSD). Sample preparation for OIM involved mechanical polishing to a mirror finish followed by ion polishing using a Hitachi 4000 plus ion polisher at 45 kV and 20 mA for several minutes. A scan step size <100 nm and electron beam diameter of 20 nm were utilized during OIM.

3. Results

Fig. 2a shows OIM of the heterogeneous surface topography from which microstructure parameters pertaining to gradients in grain diameter (δ), recrystallization fraction (f_{rx}), dislocation structure orientation and crystallographic texture were extracted. From the figure, a high concentration of UFGs was seen across the entire surface wavelength in the immediate subsurface, compared to microcrystalline grains observed at greater subsurface depths. Fig. 2b summarizes grain size $\delta_{2^{\circ}}$ measurements as a function of depth in the direction of the surface normal (d) for two locations along the surface wavelength. From the figure, the gradient in grain size was steeper for $\frac{x}{1} \sim 0.6$ in comparison to $\frac{x}{1} \sim 0.35$, wherein grain size $\delta_{2^{\circ}}$ denotes grains comprised of boundaries having misorientation greater than 2°. The gradient in grain size $\left(\frac{\partial \delta_{2^{\circ}}}{\partial d}\right)$ observed here is similar to that noted elsewhere for conventional material removal configurations [17]. Fig. 3 shows higher resolution OIM of the subsurface microstructure field. The dashed white line in Fig. 3a demarcates the zone abutting the surface exhibiting presence of UFGs with $\delta_{15^{\circ}}$ < 0.5 μ m. From the micrograph, it is clear that this UFG layer thickness d_{ufg} varied with respect to location along the surface wavelength. This variation, illustrated in Fig. 4, exhibits global and local maxima that are identified in the figure with arrows. The global maximum identified at $\frac{x}{3} \sim 0.17$ corresponds to the location approximately halfway between points A and B in Fig. 3a. The smaller local maxima at $\frac{x}{2} \sim 0.6$ corresponds to the zone within the dotted ellipse near apex B in Fig. 3a. The UFG surficial zones exhibited pancake shaped grains with serrated boundaries impinging onto the surface, identified using white arrows in Fig. 3a and magnified in Fig. 3b. These features are indicative of geometric dynamic recrystallization [27,28] wherein serrations on opposing sides of a grain impinge with imposition of incremental shear and result in formation of several offspring grains.

Extent of recrystallization was quantified by determining recrystallization fraction, given as $f_{TX} = \frac{\ell_{HAGB}}{\ell_{LAGB} + \ell_{HAGB}}$, where ℓ_{LAGB} and ℓ_{HAGB} refer to length of low and high angle grain boundaries

Download English Version:

https://daneshyari.com/en/article/7877628

Download Persian Version:

https://daneshyari.com/article/7877628

<u>Daneshyari.com</u>